

First principles study of the spin state transitions in $\text{GdBaCo}_2\text{O}_{5.5}$

V. Pardo^{1,2,*} and D. Baldomir^{1,2}

¹ Departamento de Física Aplicada, Facultad de Física, Universidad de Santiago de Compostela, E-15782 Campus Sur s/n, Santiago de Compostela, Spain

² Instituto de Investigaciones Tecnológicas, Universidad de Santiago de Compostela, E-15782, Santiago de Compostela, Spain

Electronic structure calculations were carried out on the compound $\text{GdBaCo}_2\text{O}_{5.5}$. The electronic structure variation with a change in the spin state of the Co in an octahedral environment has been studied, describing how a transition to an IS state explains the experimental findings. The orbital ordering has been described, not corresponding to any of those predicted in the literature. Big unquenched orbital angular momenta are calculated and their origin is described.

PACS numbers: 71.20.-b, 71.30.+h, 75.50.Pp

I. INTRODUCTION

Co oxides have been the objective of deep research during the last few years. As any correlated oxide, they present an interplay between the electronic structure, magnetic properties and geometric structure that makes them very interesting from both an experimental and a theoretical point of view. They have received a strong attention very recently, mainly after the discovery of both superconductivity¹ and magnetoresistance² in them because of the vast technological applications of those phenomena, but also because of the magnetic transitions accompanied of structural transitions, that are not yet fully understood. $\text{GdBaCo}_2\text{O}_{5.5}$ presents magnetic transitions at about 75 and 220 K and a metal-insulator transition at some 360 K.³ The magnetization measurements at the different phases have not been conclusively adscribed to a particular spin state and orbital configuration. There are no measurements available of the orbital magnetic moments of the Co ions in the different phases and spin states. This rich variety of phases including spin state transitions occurs in Co^{3+} compounds, where the low-spin state is not stable at all temperatures because of the small magnitude of the crystal field, comparable to the intra-atomic exchange energy. This is the case of $\text{GdBaCo}_2\text{O}_{5.5}$, that also presents giant magnetoresistance² associated with a metal-insulator transition. Very recently, a spin blockade phenomenon has been found to explain its conduction properties^{4,5} but very little has been studied from a theoretical standpoint.^{6,7} The goal of this paper is to make use of electronic structure calculations in order to explain the magnetic and electronic structure of the compound and their variations with respect to the magnetic and spin state transitions that occur in it. For doing so, in section II we will describe the structure of the material and the method of calculation, in section III we will present our calculations of the magnetic and electronic structure, dealing with the spin state, magnetic and metal-insulator transitions, and also with the orbital ordering phenomenon relating all of them to the macroscopic observations establishing a consistent picture for the observed properties of the material.

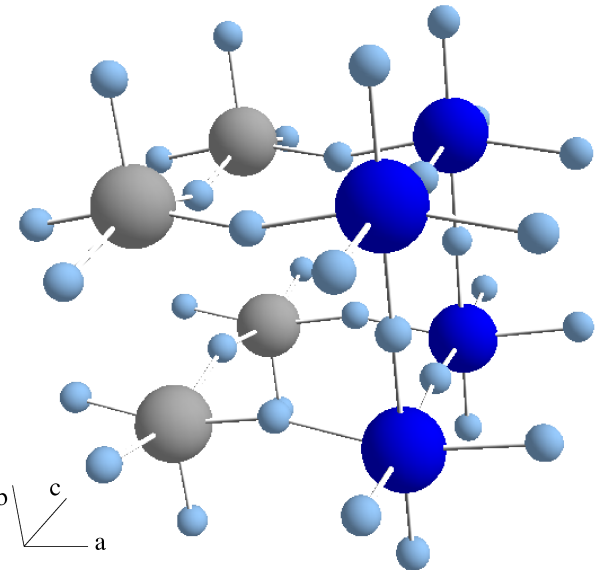


FIG. 1: (Color online) Structure of $\text{GdBaCo}_2\text{O}_{5.5}$. Dark atoms are Co_{oct} , grey atoms are Co_{pyr} and the small light ones are the oxygen atoms. Observe the oxygen vacants along the c-axis leading to a square pyramidal environment.

II. STRUCTURE AND COMPUTATIONAL DETAILS

$\text{GdBaCo}_2\text{O}_{5.5}$ presents two crystallographically different surroundings for the two inequivalent Co ions in the unit cell. One of them is in a square pyramidal (Co_{pyr}) and the other in an octahedral environment (Co_{oct}). There is one oxygen vacant per unit cell, that produces the square pyramidal environment for the Co in the crystallographic position 2r. The octahedron surrounding Co_{oct} is elongated along the a-axis (see Fig. 1 for the naming of the crystallographic directions). The unit cell is orthorhombic with space group Pmmm. The value of the lattice parameters and atomic positions were taken from Respaud *et al.*⁸ ($a = 3.87738 \text{ \AA}$, $b = 7.53487 \text{ \AA}$ and $c = 7.8269 \text{ \AA}$), but the oxygen positions were recalculated performing a full structural relaxation. It is well

TABLE I: Crystallographic positions at T= 0 that result from our structure optimization.

Atom	Crystallographic position	Coordinates
Ba	2 σ	(0,0,0.2503)
Gd	2p	(0,0.5,0.2292)
Co1	2r	(0.5,0.2563,0.5)
Co2	2q	(0.5,0.2487,0)
O1	1a	(0.5,0,0)
O2	1e	(0.5,0,0.5)
O3	1c	(0.5,0.5,0)
O4	2s	(0,0.2731,0)
O5	2t	(0,0.3102,0.5)
O6	4u	(0.5,0.2947,0.2633)

established that the oxygen vacants are in the crystallographic position 1g (1/2, 1/2, 1/2).⁸ For our calculations we broke the symmetry along the b-axis, so that 4 inequivalent Co atoms enter the cell (Co1 and Co2 in the pyramidal position, Co3 and Co4 in the octahedral environment).

We present here full potential, all electron, electronic structure calculations based on the density functional theory (DFT) utilizing the APW+lo method⁹ performed using the WIEN2k software.^{10,11} For the structure minimization, the results of which are summarized in Table I, we used the GGA (generalized gradient approximation) in the Perdew-Burke-Ernzerhoff (PBE) scheme.¹² The geometry optimization was carried out minimizing the forces in the atoms and the total energy of the system. For the electronic structure calculations we included the strong correlations effects by means of the LDA+U scheme¹³ in the so-called “fully-localized limit”.¹⁴ Spin-orbit effects have been introduced in a second variational way using the scalar relativistic approximation.¹⁵ The parameters of our calculation depend on the type of calculation but for any of them we converged with respect to the k-mesh and to R_{mt}K_{max}, up to 1000 k-points (256 in the irreducible Brillouin zone) and up to R_{mt}K_{max}=7. Local orbitals were added for a bigger flexibility in dealing with the semicore states. Muffin-tin radii chosen were the following: 2.3 a.u. for both Ba and Gd, 1.90 a.u. for Co and 1.59 a.u. for O.

III. ELECTRONIC AND MAGNETIC STRUCTURE

From a purely ionic point of view, we expect both Co³⁺ ions in a d⁶ configuration, that in an octahedral environment could lead to either a low spin (LS) state (t_{2g}⁶e_g⁰; nonmagnetic S=0) or to an intermediate spin (IS) state (t_{2g}⁵e_g¹; S=1) or even in a high spin (HS) state (t_{2g}⁴e_g²; S=2). Spin state transitions play an important role in the temperature evolution of the electronic, structural and magnetic properties of transition metal oxides, specially in the case of Co³⁺ compounds, such as the famous

case of LaCoO₃.¹⁶ In the case of GdBaCo₂O_{5.5}, it is not yet clearly understood the relationship between a spin state transition and the transition from antiferromagnetic (AF) to ferromagnetic (FM) behavior¹⁷ (neither with the metal insulator transition).¹⁸ We have studied in this paper how the electronic structure evolves with spin states and our calculations always relax to a scenario with Co_{pyr} in the IS state, as it is well established in the experimental literature.³ However, for Co_{oct}, different spin states could be converged. With these data, one can analyze how the electronic structure varies when a shift from a LS state at lower temperatures to an IS state at high enough temperatures occurs. A HS state of Co_{oct} could not be converged with the structural data we utilized. It has been shown experimentally that a structural transition⁸ occurs when a HS state sets in. This state is stabilized through a strong spin-lattice coupling that our zero temperature DFT calculations cannot describe. So, our study will be restricted to temperatures below the metal insulator transition where the HS sets in.

For the Co³⁺ ion in an octahedral environment, the purely ionic energy of the LS and IS are very close (the crystal field splitting is of the same order of magnitude as the exchange energy), and so, thermal excitations can promote the IS at sufficiently high temperatures. Co_{pyr} is located in an environment with an orbital degree of freedom, that leads to the possible existence of orbital ordering along the a-axis.^{19,20} We will deal with this issue in section III A.

We have studied several magnetic and spin configurations within the LDA+U approximation. Both FM and AF couplings along the a- and c-axes have been considered. Our calculations yield a FM coupling along the a-axis as the most stable one for any spin state. In the case of an IS for Co_{oct}, a FM coupling between Co_{oct} and Co_{pyr} is more stable than an AF one. The energy difference between both configurations is about 40 meV/Co (a strong magnetic coupling), a value that depends on U but it is qualitatively consistent for different combinations of U's.

It is difficult to discern which spin state is more stable within an LDA+U scheme, because a different spin state has its corresponding U value and these are difficult to estimate *ab initio*.²¹ We have chosen a set of U's (actually effective U, assuming J=0) that reproduce the experimentally observed situation of an IS-LS ground state. This occurs when U for Co in an IS is bigger than in the LS. The values we used are those that lead to an energy difference between the IS-LS and IS-IS configurations of about 200 K. These are: U= 4.1 eV for IS and U= 2.7 eV for LS.

From all this, we can describe the AF-FM transition due to the spin state transition in Co_{oct} from LS to IS state. This is in agreement with the experimental measurements of total magnetization, that show an effective magnetic moment of about 2.1 μ_B /Co in the ferromagnetic insulator (FMI) region²², that is consistent with the

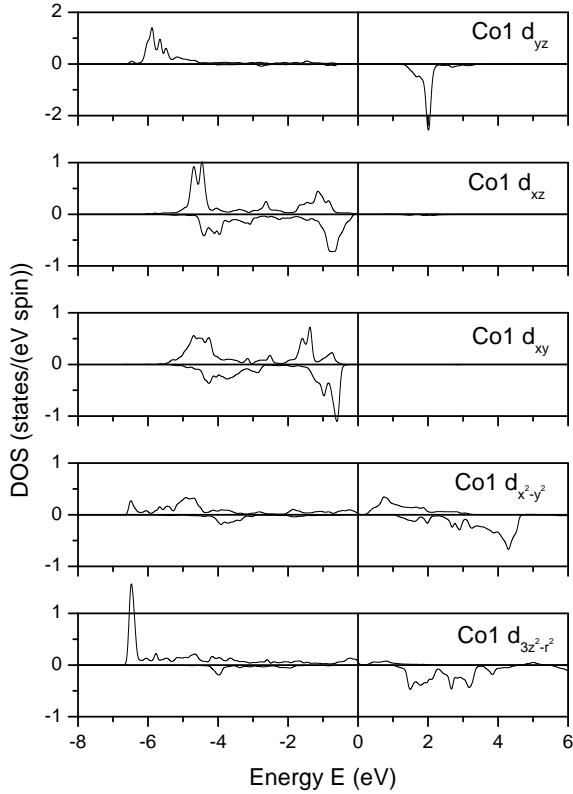


FIG. 2: Partial density of states for Co1 in the pyramidal position. It can be observed that it is in an IS state and the hole in the t_{2g} multiplet is in the d_{yz} orbital.

IS-IS scenario we propose.

A. Orbital ordering

The electronic structure of Co_{oct} presents an orbital degeneracy, that is partly lifted by the distortion of the octahedron surrounding it. This is elongated along the crystallographic c-axis (we will consider it here as our z-axis for the representation of the d-levels). For the pyramidal environment, the z-axis will be considered along the direction of the oxygen vacant (crystallographic b-axis). For Co_{pyr} , due to the small crystal field splitting a Co^{3+} ion suffers, an orbital degeneracy is likely to occur as well (depending on the intra-atomic exchange energy).

In Figs. 2, 3, 4 and 5 we can see the partial density of states (DOS) of the d-levels for the four inequivalent Co atoms considered in the unit cell.

Let us first begin with the IS-LS situation, the ground state. Figs. 2 and 3 show the DOS for the IS state of the Co_{pyr} atoms. Their electronic structure does not vary much when the spin state of Co_{oct} changes. It is

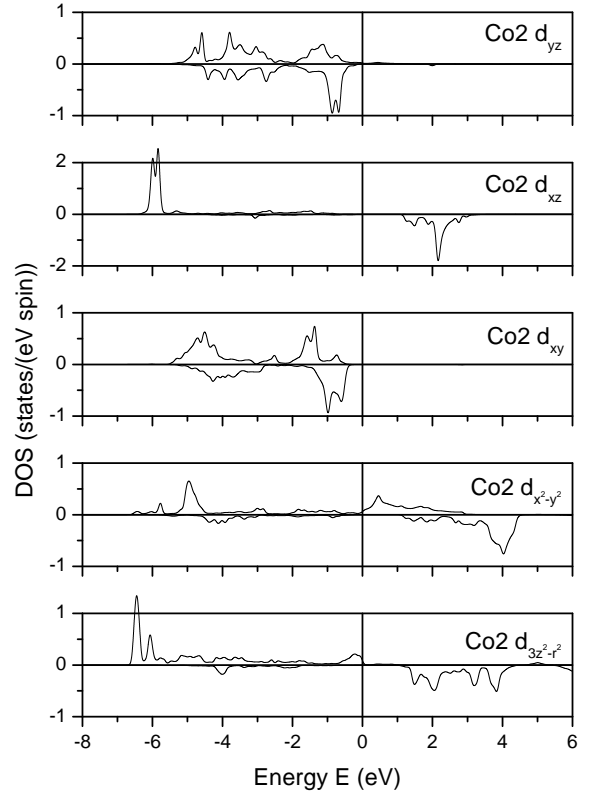


FIG. 3: Partial density of states for Co2 in the pyramidal position. It can be observed that it is in an IS state and the hole in the t_{2g} multiplet is in the d_{xz} orbital.

well established that the IS state of Co_{pyr} is fairly stable and remains unchanged when increasing temperature, so our description of this state is valid both for the IS-LS and IS-IS configurations. We can observe in the curves some kind of orbital ordering along the a-axis (the crystallographically axis that joins the two inequivalent Co_{pyr} atoms we have considered in our calculations). In Ref. 20, this orbital state is predicted to be $d_{xz} \pm i d_{yz}$ for $\text{DyBaCo}_2\text{O}_{5.5}$, but we obtain as the ground state an orbital ordering between real orbitals (d_{xz} and d_{yz}), being this configuration some 20 meV/Co more stable than the state with equal orbital structure along the a-axis (even though the magnitude of the energy difference is dependent on the value of U chosen, the important point is that it certainly is more stable independently of U). However, the location of the electron that is promoted into the e_g doublet is more difficult to adscribe, since it is not in a pure $d_{3z^2-r^2}$ nor in the $d_{x^2-y^2}$ orbital, as can be observed in Fig. 2. We also decomposed the DOS curves in a set of orbitals using the complex functions $d_{3z^2-r^2} \pm i d_{x^2-y^2}$ but the electron does not fit into those orbitals alternately neither. Some more complicated orbital

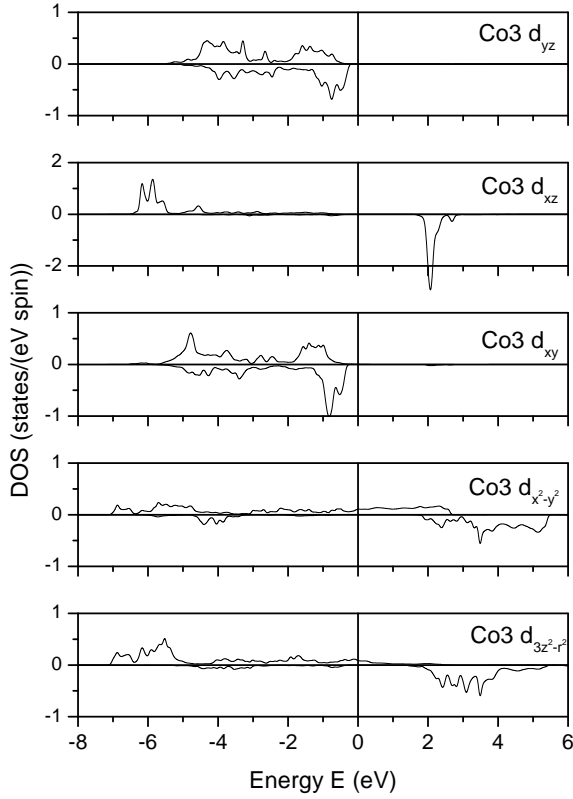


FIG. 4: Partial density of states for Co3 in the octahedral position for the IS-IS configuration. It can be observed that it is in an IS state and the hole in the t_{2g} multiplet is in the d_{xz} orbital.

structure occurs that we could not discern with our calculations, we can only ascertain that the resultant states must have some component of each orbital, probably a complex combination since an unquenched orbital angular momentum occurs as we will see below. Also, the e_g bands (this is valid for Co_{oct} in an IS state as well) contain more than one electron, that probably comes from a very strong hybridization of the e_g band with the surrounding O p bands. This could imply the formation of a $\text{Co}^{2+}\underline{\text{L}}$ state ($\underline{\text{L}}$ being a ligand hole). This strong hybridization had been already found in previous works.^{6,23}

For the case of the Co_{oct} , we present in Figs. 4 and 5 the DOS for the IS state. The plots of the LS state are not introduced because the electronic structure is basically a $t_{2g}^6 e_g^0$ configuration in a nearly octahedral environment, the t_{2g} levels fully occupied and the e_g levels fully unoccupied. It is more interesting to discuss the situation after a spin state transition from the LS to the IS state occurs on increasing temperature. One of the electrons in the lower lying multiplet is promoted to the e_g levels. There occurs an orbital ordering phenomenon as well for Co_{oct}

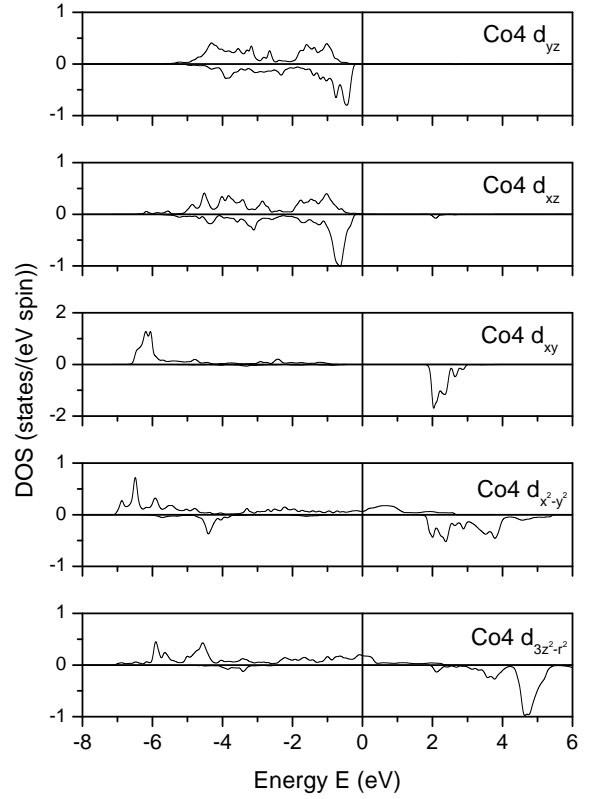


FIG. 5: Partial density of states for Co4 in the octahedral position for the IS-IS configuration. It can be observed that it is in an IS state and the hole in the t_{2g} multiplet is in the d_{xy} orbital.

in the IS state along the a-axis, the DOS of two contiguous Co_{oct} atoms along that direction are shown in Figs. 4 and 5, where it can be seen that the hole left in the t_{2g} multiplet is alternatively at the d_{xy} and d_{xz} orbitals. This configuration is some 10 meV/Co more stable than the non-orbitally ordered scenario. The electron that is promoted in the e_g multiplet places in alternate orbitals, but from our calculations it is difficult to describe the combination of $d_{3z^2-r^2}$ and $d_{x^2-y^2}$ orbitals that forms the doublet. We know it is not the pure real orbitals as we can see in Figs. 4 and 5 but they are not the complex orbitals $d_{3z^2-r^2} \pm i d_{x^2-y^2}$ either. We tried that possibility decomposing our DOS in that basis but such an ordering was not found. Some other admixture of these orbitals is happening due to the local environment of the atom but from our calculations this could not be sorted out. We encounter here a similar situation to the case of Co_{pyr} , the fact that there exist some unquenched orbital angular momenta rules out the possibility of having real orbitals, the electron must be located in a state formed by some complex combination of orbitals. The e_g band

is also in this case strongly hybridized, forming a Co^{2+}L state as for Co_{pyr} . A situation with a Co^{2+} ion in a HS state was not found according to the total magnetic moment we obtain for the whole unit cell, in contrast to the scenario proposed in Refs. 4 and 5.

In the IS-IS configuration, the material has an orbital ordering both for Co_{pyr} and Co_{oct} along the a-axis. We did not explore the orbital coupling along the b-axis (due to cell size limitations) but the picture established by Taskin *et al.*¹⁹ is qualitatively compatible with ours as far as our calculations can tell. Further studies with a doubled cell would be necessary to establish the nature of the orbital ordering along the b-axis (an alternating orbital scenario was assumed by Taskin *et al.*¹⁹) and also to study the long-range magnetic coupling between Co_{pyr} atoms mediated by the non-magnetic LS Co_{oct} and how this coupling varies when the intermediate Co_{oct} ions acquire spin.

B. Spin-orbit study: unquenched orbital angular momenta

We have also carried out calculations including spin-orbit coupling to elucidate how the magnetic anisotropy changes for the different spin states, magnetic couplings and to evaluate the orbital angular momenta (OAM) of the different Co atoms in the structure, that had been predicted to have some unquenched OAM²⁰ but whose values have never been measured. Only values of total magnetization are available in the literature,^{17,24,25} showing some discrepancies between them.

TABLE II: Values of the orbital angular momenta of the four Co atoms in the structure in the two spin state configurations studied. The values are given in μ_B and are considered inside the muffin-tin sphere. These values are calculated for the magnetization along the experimental easy axis.

Atom	IS-IS (μ_B)	IS-LS (μ_B)
Co1 (pyr)	0.30	0.28
Co2 (pyr)	0.02	0.01
Co3 (oct)	0.01	-0.05
Co4 (oct)	0.24	-0.07

A summary of the OAM calculated is presented in Table II. The values are given inside the muffin-tin spheres, so the real values of the moments are, hence, somewhat bigger (about 10-30%, but this is difficult to estimate). These data presented here are calculated assuming the magnetization goes along the experimental easy axis (a-axis). These values are U-dependent by up to 25% for other combinations of U parameters within a reasonable range. Large values up to $0.6 \mu_B$ for some of the Co atoms would be consistent with our calculations. Experimental measurements are needed to confirm this observation. Irrespective of the Co_{oct} spin state, we observe that Co_{pyr} atoms have very similar angular momenta (about $0.3 \mu_B$ inside the muffin-tin sphere). The electronic structure of

these atoms barely changes when a spin state transition occurs to Co_{oct} . This atom develops a big angular momentum in one of the sites when it is in an IS state. It is worth noting that the big orbital angular momentum occurs when the hole in the t_{2g} multiplet is left in the d_{xz} orbital, both in the case of Co_{pyr} and Co_{oct} in an IS state, whereas the configuration with a hole in a different t_{2g} orbital produces a negligible moment. Small values are predicted also for Co_{oct} in a LS state, oppositely oriented to the magnetic moment of the Co_{pyr} ions. The magnetization in that case comes only from this angular contribution.

We also performed calculations of the magnetic anisotropy energies and our results strongly disagree with the experimental data available¹⁹. For the IS-LS state, we find a hard axis along the c-axis, being the a and b directions easier by some 20 K/Co. No trace of Ising-like behavior was found. Also, for the IS-IS state, the b-axis is the easy axis being the a and c directions harder by some 20 K/Co. This implies a change in the ordering of easy directions (not in the easy axis) with a change in spin state, that has been ruled out experimentally.¹⁹ The explanation for this discrepancy could be that the origin of the strong Ising-like behavior is not magnetocrystalline anisotropy but some shape anisotropy induced by domain formation in the material. This situation contrasts with other related compounds, such as $\text{Ca}_3\text{Co}_2\text{O}_6$, where the Ising-like behavior was shown to have magnetocrystalline origin by similar calculations.²⁶

C. Magnetic ordering and magnetic transitions

From our calculations, we interpret the AF-FM transition that occurs at about 220 K related to the spin state transition on Co_{oct} . The magnetic coupling between Co_{oct} and Co_{pyr} being both in an IS state is FM, whereas for the case of the LS-IS configuration, the experimentally found AF ordering between FM planes of Co_{pyr} separated by nonmagnetic Co_{oct} layers is consistent with our calculations. Also, in the IS-LS configuration, there is an AF coupling between Co_{pyr} and a very small orbital contribution to the magnetic moment of the adjacent Co_{oct} polarized opposite to it (see Table II).

Finally, with the aid of the total DOS plots in Fig. 6 we can address the problem of the subsequent transitions that occur in the system. We observe that the IS-LS is a zero-gap insulator, in accordance with experiments observing a narrow gap.¹⁹ However, the IS-IS configuration is half-metallic according to our calculations. This would contradict the fact that a FMI phase appears at temperatures below the metal-insulator transition but it could be an artifact of the calculations since we are not including the orbital ordering along the b-axis assumed in Ref. 19 due to limitations of our unit cell. This symmetry break could further split the d-bands crossing the Fermi level that we consider degenerate, but more calculations are necessary to confirm this point. A scenario with an IS-IS

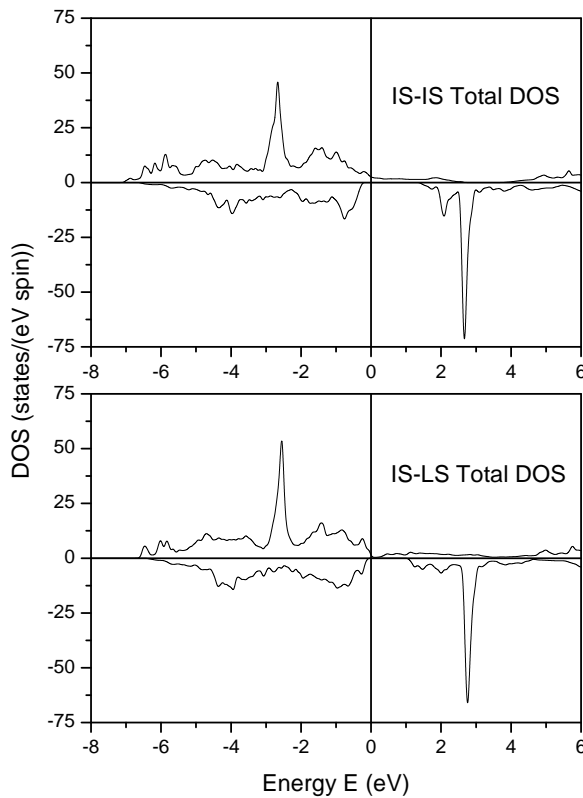


FIG. 6: Total DOS plots for the material in the two spin states considered in the text. Observe that it is an insulator in an IS-LS state but it becomes half-metallic when it is in an IS-IS state at higher temperatures, a fact that is probably an artifact of the calculations that do not consider the orbital ordering along the b-axis.

FM state could explain the properties of the FMI phase. In our picture, an AF-FM transition occurs due to a spin state transition in the Co_{oct} and the transition to a HS state comes accompanied of a drastic change in conduction with the appearance of a metal-insulator transition.

From our calculations, the orbital ordering is a very stable situation. Without considering it along the b-axis, that would make it even more stable, a stabilization energy of more than 200 K was found. Hence, our calculations are consistent with the finding of orbital ordering for temperatures below the metal-insulator transition.

IV. CONCLUSIONS

In this paper we have presented a study of the electronic structure and magnetic properties of the Co oxide $\text{GdBaCo}_2\text{O}_{5.5}$ using *ab initio* calculations considering an all-electron, full-potential APW+lo method. The points we tried to address were the spin state transitions, the orbital ordering and spin-orbit effects. From our calculations we confirmed several well established experimental facts, such as the stability of the IS state for Co_{pyr} or the conduction properties of the IS-LS state as a narrow gap insulator. We have observed the material is in an orbitally-ordered state both at low temperatures in the IS-LS state and also at higher temperatures when transiting to an IS-IS state, and we described the orbitals involved in the phenomenon. We also predict big unquenched orbital angular momenta for some of the Co atoms in the structure, a fact that had been predicted but whose values have never been measured. We estimate their values and explain their origin. The subsequent transitions the material undergoes with temperature can all be explained with our results. In summary, we establish a consistent picture for the properties of the material by confirming some experimental evidences and predicting new results based on first principles calculations.

Acknowledgments

The authors wish to thank the CESGA (Centro de Supercomputación de Galicia) for the computing facilities and the Xunta de Galicia for the financial support through a grant and the project PGIDIT02TMT20601PR.

* Electronic address: vpardo@usc.es

¹ K. Takada, H. Sakurai, E. Takayama-Muromachi, F. Izumi *et al.*, *Nature (London)* **422**, 53 (2003).

² C. Martin, A. Maignan, D. Pelloquin, N. Nguyen *et al.*, *Appl. Phys. Lett.* **71**, 1421 (1997).

³ A.A. Taskin, A.N. Lavrov, and Yoichi Ando, *Phys. Rev. B* **71**, 134414 (2005).

⁴ A. Maignan, V. Caignaert, B. Raveau, D. Khomskii *et al.*, *Phys. Rev. Lett.* **93**, 026401 (2004).

⁵ A.A. Taskin and Yoichi Ando, *cond-mat/0509673* (2005).

⁶ Hua Wu, *J. Phys.: Condens. Matter* **15**, 503 (2003).

⁷ Qinfang Zhang and Weiyi Zhang, *Phys. Rev. B* **67**, 094436 (2003).

⁸ C. Frontera, J.L. García-Muñoz, A. Llobet, and M.A.G. Aranda, *Phys. Rev. B* **65**, 180405(R) (2002).

⁹ E. Sjöstedt, L. Nördstrom, and D.J. Singh, *Solid State Commun.* **114**, 15 (2000).

¹⁰ K. Schwarz and P. Blaha, *Comp. Mat. Sci.* **28**, 259 (2003).

¹¹ P. Blaha, K. Schwarz, G. K. H. Madsen, D. Kvasnicka *et al.*, *WIEN2k, An Augmented Plane Wave Plus Local Orbitals Program for Calculating Crystal Properties. ISBN 3-9501031-1-2*, Vienna University of Technology, Austria

(2001).

¹² J.P. Perdew, K. Burke, and M. Ernzerhof, Phys. Rev. Lett. **77**, 3865 (1996).

¹³ A.I. Lichtenstein, V.I. Anisimov, and J. Zaanen, Phys. Rev. B **52**, R5467 (1995).

¹⁴ A.G. Petukhov, I.I. Mazin, L. Chioncel, and A.I. Lichtenstein, Phys. Rev. B **67**, 153106 (2003).

¹⁵ D.J. Singh, *Planewaves, pseudopotentials and LAPW method* (Kluwer Academic Publishers, 1994).

¹⁶ M.A. Korotin, S.Yu. Ezhov, I.V. Solovyev, V.I. Anisimov *et al.*, Phys. Rev. B **54**, 5309 (1996).

¹⁷ W.S. Kim, E.O. Chi, H.S. Choi, N.H. Hur *et al.*, Solid State Commun. **116**, 609 (2000).

¹⁸ C. Frontera, J.L. García-Muñoz, A. Llobet, M.A.G. Aranda *et al.*, J. Alloy Compd. **323-324**, 468 (2001).

¹⁹ A.A. Taskin, A.N. Lavrov, and Yoichi Ando, Phys. Rev. Lett. **90**, 227201 (2003).

²⁰ H.D. Zhou and J.B. Goodenough, J. Solid State Chem. **177**, 3339 (2004).

²¹ G.K.H. Madsen and P. Novak, Europhys. Lett. **69**, 777 (2005).

²² Z.X. Zhou, S. McCall, C.S. Alexander, J.E. Crow *et al.*, Phys. Rev. B **70**, 024425 (2004).

²³ W.R. Flavell, A.G. Thomas, D. Tsoutsou, A.K. Mallick *et al.*, Phys. Rev. B **70**, 224427 (2004).

²⁴ M. Respaud, C. Frontera, J.L. García-Muñoz, M.A.G. Aranda *et al.*, Phys. Rev. B **64**, 214401 (2001).

²⁵ S. Roy, M. Khan, Y.Q. Guo, J. Craig *et al.*, Phys. Rev. B **65**, 064437 (2002).

²⁶ Hua Wu, M.W. Haverkort, D.I. Khomskii, and L.H. Tjeng, cond-mat/0504490 (2005).